Cavity Air Flow Behavior During Filling in Microinjection Molding

C. A. Griffiths[1]
S. S. Dimov
S. Scholz

Cardiff School of Engineering,
Cardiff University,
Queens Building,
Cardiff, CF24 3AA, UK

G. Tosello
Department of Mechanical Engineering,
Technical University of Denmark,
Kgs. Lyngby DK2800, Denmark

Process monitoring of microinjection molding (μ-IM) is of crucial importance in understanding the effects of different parameter settings on the process, especially on its performance and consistency with regard to parts' quality. Quality factors related to mold cavity air evacuation can provide valuable information about the process dynamics and also about the filling of a cavity by a polymer melt. In this paper, a novel experimental setup is proposed to monitor maximum air flow and air flow work as an integral of the air flow over time by employing a microelectromechanical system gas sensor mounted inside the mold. The influence of four μIM parameters, melt temperature, mold temperature, injection speed, and resistance to air evacuation, on two air flow-related output parameters is investigated by carrying out a design of experiment study. The results provide empirical evidences about the effects of process parameters on cavity air evacuation, and the influence of air evacuation on the part flow length. [DOI: 10.1115/1.4003339]

Keywords: microinjection molding, process monitoring

1 Introduction

Micro-/mesoscale components and products are gaining an increasing importance in areas such as the health care, IT, communication, medical, pharmaceutical, consumer goods, and automotive sectors. In addition, microtechnologies are predicted to play an important role in interfacing macro- and nanoworlds, and thus in the development of new miniaturized products including a range of medical and biotechnology applications [1,2]. There are significant technological advances in the area of microfabrication [3,4] and one of the key technologies identified is microinjection molding (μ-IM). This replication technique is a reliable and cost effective means of producing a wide range of microcomponents in thermoplastics such as optical grating elements, micropumps, microfluidic devices, and microgears in large quantities.

μ-IM can be defined in general terms as a process for producing polymeric parts with functional features/structures in the micron or submicron range [5,6]. Yao and Kim [7] proposed the components manufactured by μ-IM to be clustered into one of the following two main categories. Type A are components with overall sizes of less than 1 mm while Type B have larger overall dimensions but incorporate microfeatures with sizes typically smaller than 200 μm. In addition, Kukla and Loibl [8] suggested that μ-IM could also cover parts of any dimensions with a mass in the order of a few milligrams.

At the same time it is important to acknowledge that there is a rich repository of polymer processing knowledge for injection molding (IM). However, due to scale effects, such know-how cannot be employed directly in μ-IM, and also some proven designs and processing strategies at macroscale should be carefully reconsidered taking into account these scale effects [9]. μ-IM uses a plasticizing method that differs to standard screw type machines. In particular, a combination of fast servodrives and mechanical parts ensures extremely short switchover times of 2.5 ms at an injection speed of 1000 mm/s. With low filling times the polymer volume can be difficult to control, and therefore it is not surprising that many researchers have focused their attention on the filling stage of the process [10–13]. The results from the carried out literature review indicate that high settings for injection speed (V_i) and hence injection pressure (P_i), together with temperature (T) factors, such as melt and mold temperatures, can be used to counteract the short freezing time and thus to extend the flow length of polymer melts when filling microcavities [14].

In this research the focus will be on the factors that influence the air evacuation (E_a) from the cavity during the filling stage. One of the most important conditions for consistent replication is the evacuation of air or gas from the cavity. Inadequate E_a in the mold can result in air pockets trapped against the cavity walls and/or between converging flow fronts. This can cause problems such as burn marks and short shots [15]. In particular, burning conditions can arise from an air subjected to an adiabatic temperature change, the extreme of which is when P and T are high enough to cause the air to ignite and burn the polymer. In addition, short shots can be caused by an air that failed to evacuate and remained trapped into an unfilled area of the cavity. Such trapped air can resist the melt flow and lead to an excessive cavity pressure that can be necessary to fill the cavity completely. Thus, E_a is required to improve part quality and also to prevent tool damage.

One important design solution for reducing air traps is venting. Ideally vents are present at the mold split lines; however, often it is required to position them in areas of converging flow fronts and last-to-fill flow fronts of the cavity. In designing vent systems for macroscale components it is necessary to consider the relationship between T and P in cavities. This is required in order to prevent the filling of vent gaps that can result in an excess polymer on the molded part and further processing steps for flash removal [16]. In particular, the permissible width of the vent gaps, which prevents the melt from entering them, depends primarily on the time between the first contact the melt has with the vent area and the rise in P [17]. The critical gap widths for polymer materials range from 15 μm to 30 μm, and typically a vent can be about 25 μm deep and several mm wide [18]. For μ-IM such vent sizes could be comparable with some of the functional features of the molded microparts, and thus it will be difficult and even impossible to prevent their filling by the melt flow due to relatively high process settings in microinjection molding.

In addition to changing vent dimensions, the air flow rate ($\dot{Q}$) at the vent exit can be considered. Traditionally, a reduction in the machine clamp force, and the use of a suitable V_i profile can change $\dot{Q}$ and allows more time for E_a. However, the high accuracy of the molds and the high V_i requirements in μ-IM mean that the applicability of existing methodologies and solutions for vent-

[1]Corresponding author.

Contributed by the Manufacturing Engineering Division of ASME for publication in the JOURNAL OF MANUFACTURING SCIENCE AND ENGINEERING. Manuscript received July 27, 2010; final manuscript received December 21, 2010; published online January 24, 2011. Assoc. Editor: Lih-Sheng (Tom) Turng.

ing should be reconsidered. Taking this into account one solution suggested was to apply a negative vacuum at the vent exit [19]. The trade offs in selecting an appropriate position for the vents as far as possible from the optimized location of the gate require extensive experimentation mostly on a trial and error basis [20]. Therefore, each potential solution should be considered taking into account all relevant aspects of the molding process.

The performance of the μ-IM process is highly dependent on E_a as an important prerequisite for the production of quality parts and also for prolonging the tool life. Therefore, this paper investigates the cavity $\dot{Q}$ behavior during the filling stage in μ-IM, with a particular focus on the inter-relationship between process settings and $\dot{Q}$ during E_a. The paper is organized as follows. Section 2 discusses important factors related to air presence in mold cavities. Then, the experimental setup, the test tool, and the condition monitoring techniques used to investigate the effects of the process parameters on the $\dot{Q}$ behavior are described in Sec. 3. Next, in Sec. 4, the design of experiments for conducting the proposed research is discussed. The experimental results are presented and the relationship between process parameters and E_a in microcavities is analyzed. Finally, in Sec. 5, the main conclusions from the conducted study and recommendations for improving the μ-IM process and the quality of injection molded products by using optimal E_a settings are presented.

2 Air Presence in Mold Cavities

2.1 Venting and Vacuum. When a polymer is injected in a cavity the incoming melt has to replace the resident air. Ideally the resident air evacuates by finding the easiest way to escape. For parts with different thicknesses the nonuniform, diverging, or converging behavior of the polymer and air flows makes the positioning of injection gates and E_a vents an important design consideration, particularly for controlling the P levels during the filling stage of the process [21]. Shen et al. [22] investigated the μ-IM process for the fabrication of microlens arrays and concluded that the melt front had been filling first the thicker section of the cavity before filling the microstructures. Also, it was observed that the remaining air in the microstructures if not evacuated resulted in not completely filled parts, commonly known as short shots. The air trapped within the cavity influences the thermal interactions between the polymer melt and the mold. During the cooling cycle heat conduction takes place between the polymer surface and the mold. If there is an air gap present, the polymer surface reheats because the heat transfer is restricted. As a consequence of this polymers can exceed their critical temperatures, and also the air gap can lead to cooling variations that can result in part warpage [23]. Currently, changes in the processing conditions triggered by altering the injection locations and V_i profiles are used to prevent air traps. However, taking into account the relatively short injection time frames in the range 100 ms in μ-IM, E_a becomes a key consideration in the mold design [24].

Venting is one of the methods for achieving E_a. Ideally, the primary vent is present at the parting plane or split line of the mold faces but in spite of this nonuniform filling, patterns, hesitation effects, and insufficient gaps between the split lines can result in trapped air. In such cases secondary vents are introduced to facilitate E_a. To improve the efficiency of the vents, the exit P can be modified by applying a vacuum or negative P to the vent exits. Yoki et al. [25] investigated transcription ratio (TR) using ultrahigh speed injection molding and found out that there was a correlation between TR and V_i, flow patterns, and vent conditions. The use of a vacuum pump to facilitate E_a did not lead to noticeable improvements of replication results in comparison to those achieved employing conventional vents. However, the vacuum pump increased the average TR. For molding diffractive optics with 0.5–1 μm gratings, Kalima et al. [26] considered E_a as a process factor, and a vacuum pump was used to remove any trapped air from the mold. The study concluded that the existence of vacuum improved the filling for all studied materials. However, trapped air was still present inside the cavities and possibly contributed to not complete filling of some of the structures even when the vacuum unit was employed. Sha et al. [11] investigated the importance of E_a as a control parameter in microcavities. The results showed some improvements in part filling and surface quality; however, E_a could also lead to a decrease in the surface temperature in microchannels as a result of taking away warm air from the cavity. Therefore, for polymers that are sensitive to T_m settings, the melt fill decreases when vacuum is applied. Liou and Chen [27] used a continuous vacuum in a mold cavity and runner to keep the pressure under 1 mbar before filling, and thus to reduce the influence of temperature variations.

In conclusions, it can be stated that the use of vents and vacuum to remove air traps can have both positive and negative effects on the μ-IM process. The specific process requirements suggest that in order to achieve an adequate E_a it is necessary to consider all relevant tool design and process factors.

2.2 Weld Lines. Another area where ineffective E_a can have detrimental effects on part quality is the formation of weld lines. Weld lines are usually formed when two or more flow fronts meet and converge during the part filling stage. They are unavoidable when either the flow fronts separate and reconverge or the melts come from more than one gate. Such lines can result in a mechanical weakness, visual defects, or incompletely filled cavities.

Weld line strength is generally influenced by T at which the weld line is formed. As soon as the melt enters the cavity it begins to cool and T may not be sufficient for two melt fronts to bond perfectly together when they meet. Also, residual stresses can occur due to flow fronts having different T. It was shown that aberrations in molecular orientation due to differing viscosity of two melt fronts can cause bad entanglements when they meet and thus lead to the formation of weld lines. Additionally, a compatibilizer that results in finer polymer morphology was found to increase the weld line strength [28,29]. Debondue et al. [30] identified a direct relationship between the molecular diffusion, in particular, different entanglement densities, and fracture mechanisms of weld lines that were influenced not only by the material and processing parameters but also the mold surface roughness and E_a capability.

To avoid varying T, and thus the occurrence of differential shrinkage during solidification, Michaeli and Ziegmann [31] adopted a variotherm heating of cavities before injecting, and then cooling down before demolding to prevent weld lines' formation. Liu et al. [32] used different geometric shapes as flow obstacles to investigate weld line formation and strength. From the set of process parameters investigated in this experimental study T_b and T_m were found to be the principle factors affecting the weld lines' formation and their properties. Wu et al. [33] reported that weld lines' formation could be reduced by applying higher settings for V_i, T_b, and T_m, while T_b was found to be the most influential factor. Tosello et al. [14] used weld lines as flow markers to investigate the filling performance in μ-IM, and the results showed that T_b and V_i were the most influential parameters.

Currently, in most cases the trial and error approach is used to identify process settings that can be applied to control weld lines' formation. However, with the need for higher T and V_i in μ-IM, it should be noted that such settings also intensify the occurrence of adiabatic conditions, localized air temperature increases, in the mold, and hence the requirements for and an increase in the rate of E_a.

2.3 Adiabatic Processes. The specific process conditions in μ-IM suggest that the development of appropriate E_a solutions require all relevant tool design and molding process factors to be reconsidered in a new context. Air traps within converging flow fronts or against cavity walls can lead to problems such as burn marks and surface defects. Burning conditions can arise due to air

being subjected to an adiabatic temperature change, the extreme of which is when the air pressure is sufficiently high to ignite the air and burn the plastic, i.e., causing polymer degradation.

Considering the polymer flow in a mold, the specific volume (V) of polymers varies with P and T. In particular, V increases with the decrease in P and the increase in T. The functional dependence between the polymer volume and T and P can be represented with pressure-volume-temperature (PVT) data that represent material compressibility of melt flows [34,35]. If the total amount of heat in a given V of trapped air is held constant, then when the air is compressed, its T rises. This is called adiabatic heating, and the T increase attained when work is performed on the system is called adiabatic temperature. The T increase in the air during compression tends to increase P to compensate the decrease in V, and therefore, P during adiabatic compression rises faster while V diminishes.

The ideal gas law describes the relationship between P, V, the number of moles (n), and T of an ideal gas. The state equation of a hypothetical ideal gas reflects the fact that a given number of its atoms occupy the same V, and that V changes are inverse to P change, and linear to T changes. Thus, the state of a given amount of gas is determined by its P, V, and T. Their functional dependence can be expressed analytically as follows:

$$P \cdot V = n \cdot R \cdot T \tag{1}$$

where R is the value of universal gas constant. For an adiabatic process T can be defined as follows:

$$T_2 = T_1 \cdot \left(\frac{V_1}{V_2}\right)^{y-1} \tag{2}$$

while P as

$$P_2 = P_1 \cdot \left(\frac{V_1}{V_2}\right)^{y} \tag{3}$$

where T_1, P_1, and V_1 are the initial state values and T_2, P_2, and V_2 are the final state values. y is a constant that depends on the type of gas used, and is related to the degrees of freedom of the gas molecules. For a diatomic gas such as nitrogen and oxygen, the main components of air, y is about 7/5; however, y is not constant as heat capacity changes with changes in V and P. However, it is reasonable to assume a constant y when there are only small changes in the states.

Potentially, adiabatic conditions can cause combustion within the mold cavity. The diesel effect and diesel cycle are adiabatic effects in injection molding of polymers [36]. The diesel cycle includes the following stages:

1. injection of the polymer compresses the resident air in the cavity
2. the volume of air experiences an adiabatic temperature increase
3. the air ignites
4. the air expands adiabatically

The diesel reaction occurs when an explosive mixture of gas and the processed material is formed during compression. Such a mixture results in a material volatility, which entails chemical reactions leading to the formation of a volatile gas or vapor that can etch the tool material [37]. In particular, the theoretical or the stoichiometric amount of air is the minimum amount of air that provides sufficient oxygen for the ignition of all combustible chemical elements. In most combustion applications, air provides the necessary oxygen. In combustion calculations, air is considered to contain 21% oxygen and 79% nitrogen. With such idealization the molar ratio of nitrogen to oxygen is 3.76 in combustion air. Also, nitrogen present in the air is considered inert; however, the air can be ignited due to the additional gasses released from the heating up of the polymer melt. Data obtained with a gas chromatograph device can be used to determine the composition of gaseous products of the combustion [38].

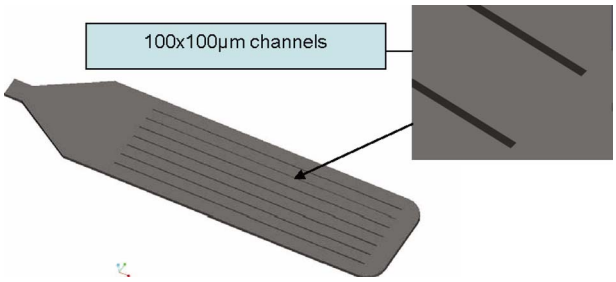

Fig. 1 Part design

In μ-IM the T settings can exceed those used in conventional IM. In particular, high T_b can improve the polymer flow while high T_m leads to a more uniform distribution of residual stresses in molded parts [39]. However, high T and V_i settings can also result in uneven melt fronts, gas traps, and burning of the molded polymers [40]. Increasing T_b, T_m, and V_i improves the polymer melt filling of microcavities, though in some cases the part edge definition can be compromised. One explanation for this could be that the expanding residual air was not vented completely and hindered the melt flow [41]. Liou and Chen [27] observed residual cavities of air in submicron structures with high-aspect ratios. The cavities were filled by gas produced at high P, and this can be regarded as being created by the gasification of the polymer. The gasification of the polymer was caused by its excessive T increase. This phenomenon was exhibited in all cases where T_m was 160°C or above and was more serious at higher T_m. At high V_i, a system for a visualization analysis established that the gas bubbles generated in unstable asymmetric melt fountain flows expanded and collapsed in contact with the tool cavity walls, which caused defects such as flow marks and silver streaks [25]. Yuan et al. [42] identified that during injection when trapped air was compressed T could increase and as a result to degrade thermally the polymer. Ruprecht et al. [43] used E_a to prevent the burning of plastic caused by the diesel effect. While Ebnesajjad [44] identified that adiabatic compression during polymer processing can raise T significantly, to about 800°C, which can degrade the plastic and can produce a by-product that will corrode the tool material.

3 Experimental Setup

3.1 Test Part Design. The test part design used in this study to analyze E_a in a cavity during injection molding is a 5 mm $\times$21 mm$\times$250 μm microfluidics platform (Fig. 1). The design includes seven microchannels with cross sections of 100 $\times$100 μm^2 and 14 mm in length. The part surface area is 226.5 mm^2 and the volume is 18.7 mm^3.

3.2 Test Materials. A commonly used material in injection molding, acrylonitrile butadiene styrene (ABS), is selected to conduct the planned experiments. Its properties are provided in Table 1. The polymer went through desiccant drying and dehumidifying

Table 1 Polymer material properties

Material	Magnum 8434
Category	ABS
Structure	Amorphous
Moldflow viscosity index[a]	VI(240)0166

[a]The number in the brackets refers to the material melt temperature (°C) while the other four digits signify its viscosity (Pa s) measured at a shear rate of 1000 (1/s).

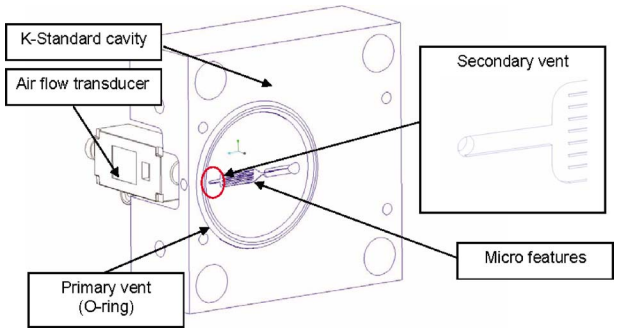

Fig. 2 Tool design

cycles before the trials to remove any surface or absorbed moisture. The machine used to perform the microinjection molding trials was Battenfeld Microsystem 50.

3.3 Mold Manufacture. The tool used to perform the experiments uses a Hasco K-standard modular system of machined and drilled plates. However, the standard system was modified to integrate an air flow transducer. The tool halves were assembled and then inspected for parallelism and shut off of the mating faces. Any gap between these faces is considered as a primary vent for E_a during polymer injection. The surface mapping of the K-standard cavity block performed with an interferometric profiling microscope revealed a roughness variation of Rz 8.6 μm, which with two mating plates would provide an air gap of up to 17.2 μm. Therefore, to control the amount of E_a from the cavity through such a primary vent, a circular channel is machined to accommodate a 4 mm diameter O-ring (46 mm inside diameter). The O-ring surrounds the cavity and seals the shut off faces, and thus restricts E_a through the primary vent.

The 3 mm diameter half round runner, gate, and micropart cavity, as shown in Fig. 2, are machined on the moving half of the mold by micromilling. At the end of the flow path, in particular, as far as possible from the gate, a secondary vent, 1 mm $\times$ 5 mm $\times$ 200 μm, is machined on the cavity face. This vent leads to a 1 mm diameter air relief orifice, through which E_a from the cavity is channeled to a sealed air flow transducer. This experimental setup allows the influence of air evacuation on the part flow length in μ-IM to be investigated, especially the filling of microparts and the $\dot{Q}$ variations of E_a.

3.4 Condition Monitoring. Condition monitoring techniques are used in μ-IM to quantify natural variations that can occur during molding cycles, and thus to identify interdependences between the resulting part quality and various tool, material, and process factors. In this study, $\dot{Q}$ variations in the cavity area were investigated using an air flow transducer, Omron D6F-01A1-110, as shown in Fig. 3. This supersensitive gas flow sensor based on a proprietary microelectromechanical system (MEMS) technology is used to measure accurately low $\dot{Q}$ over a wider range of T. In particular, the extreme sensitivity of this sensor is achieved with thermopiles that can be used to measure T or radiant energy, and then to convert them into an electric signal [45]. Inside each sensor there is a highly sensitive MEMS flow chip with dimensions $1.55 \times 1.55 \times 0.4$ mm^3. The chip has two thermopiles on the either side of a heater element used to measure the deviations in heat symmetry caused by the passing gas flow. A thin layer of insulating film protects the chip from direct exposure to the gas. When there is no $\dot{Q}$ present, the T distribution around the heater is uniform and the differential voltage of the two thermopiles is 0 V. When $\dot{Q}$ is present, the side of the flow sensor facing the source of the air flow cools and the opposite side warms, and thus unsettling the T equilibrium. The difference in T appears as a differential

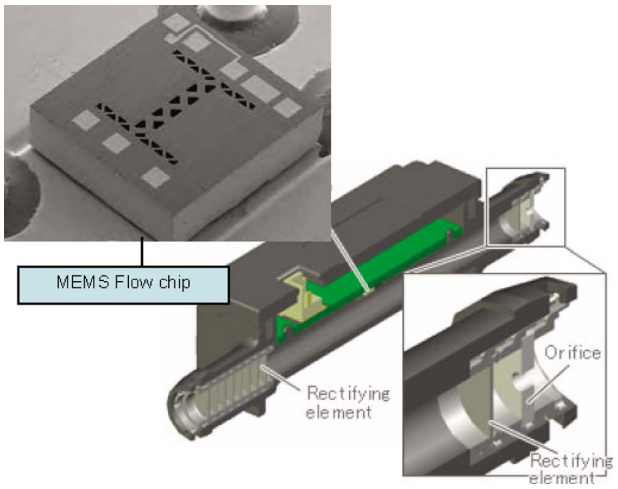

Fig. 3 Air flow transducer

voltage between the two thermopiles, and thus allowing $\dot{Q}$ to be calculated.

A National Instruments cDAQ-9172 USB data acquisition unit was utilized to analyze sensor output signals on a computer employing the National Instruments LABVIEW 8 software. When the gas sensor is subjected to $\dot{Q}$, this results in an electrical output. Ultimately, the output signal is monitored employing a National Instruments NI 9205 16 bit module. In this study the effects of the process parameters were analyzed by using this condition monitoring experimental setup, and thus to be able to measure the maximum flow rate, $\dot{Q}_{\max}$ (ml/s), and calculate the integral of Q (ml). $\dot{Q}_{\max}$ is monitored in order to determine the peak $\dot{Q}$ value that the gas sensor has experienced. This value is the maximum of $\dot{Q}$ over t where $t_{\max}$ represents the time when $\dot{Q}$ in the cavity reaches its maximum.

$$\dot{Q}_{\max} = \dot{Q}(t_{\max}) = \max(\dot{Q}(t)) \tag{4}$$

The total air flow over time, Q, determines $\dot{Q}$ over the whole duration of the filling stage and is the integral of $\dot{Q}$. Due to the fact that the $\dot{Q}$ curve, Fig. 4, is defined by the measured discrete values, Q is the sum of $\dot{Q}$ from the start of the filing stage, t_{start}, until its completion, t_{end}, multiplied by a time step of Δt. The chosen time step Δt is 1 ms and is determined by the sampling rate of the data acquisition system. Thus, Q is calculated employing the following equation:

$$Q = \left(\sum_{t=t_{\text{start}}}^{t_{\text{end}}} \dot{Q}(t) \right) \cdot \Delta t \tag{5}$$

3.5 Design of Experiments. To investigate the effects of the μ-IM process on part replication this experimental research was focused on $\dot{Q}$ of E_a, and the part flow length. The replication performance of microcavities is highly dependent on the P and T control during injection, and therefore the effects of T_b, T_m, and V_i have been investigated in this study. Additionally, the resistance to air evacuation (E_a^R) from the cavity is an important aspect that can affect the process performance. As four factors at two levels were considered, a Taguchi L16 orthogonal array (OA) was selected, as shown in Table 2.

The melt temperature was controlled through T_b and was within a recommended processing window. Two levels, maximum and minimum temperatures, were used for the polymer. In μ-IM the polymer solidification time is much shorter than that in conven-

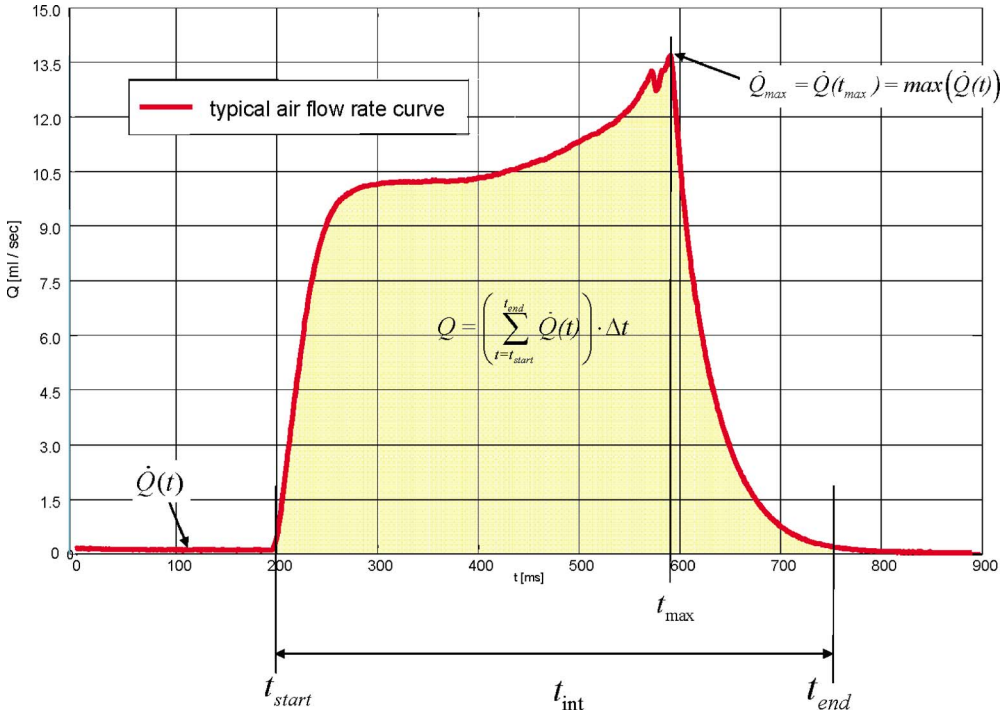

Fig. 4 A sample air flow curve

tional molding. The T_m settings used in this research were the two extremes, the minimum and the maximum values, within the recommended range for the material.

V_i has two main effects. It can help polymers to fill the cavities before the melt flow solidifies. The two levels of V_i selected in this research were chosen by taking into account the capabilities of Battenfeld Microsystem 50. The two levels of E_a^R were investigated with the help of the O-ring, in particular, the low setting is a tool without the O-ring, and the high setting is the tool with it. For each combination of controlled parameters for the selected L16 OAs, as presented in Table 2, ten runs were performed and in total $10 \times 16 = 160$ experimental trials were carried out. The response variables considered are $\dot{Q}_{max}$, Q, and part flow length.

4 Analysis of the Results

4.1 Average $\dot{Q}_{max}$, Q, and Flow Length. In this study, a L16 OA was employed to ensure that the experimental results were representative of the considered processing windows for the selected material. For each trial, the effects selected combinations of process parameters/factors on $\dot{Q}_{max}$, Q, and flow length were investigated, and then based on the conducted 160 trials the mean values were calculated for each of the 16 different processing conditions.

The quantitative $\dot{Q}_{max}$ data obtained through the experiments identified that the highest recorded $\dot{Q}_{max}$ was 40.5 ml/s, and the

Table 2 Taguchi L16 orthogonal array

	Factors							
	T_b (°C)		T_m (°C)		E_a^R **(on/off)**		V_i (mm/s)	
Run	Level	Setting	Level	Setting	Level	Setting	Level	Setting
1	1	210	1	30	1	Off	1	200
2	1	210	1	30	1	Off	2	800
3	1	210	1	30	2	On	1	200
4	1	210	1	30	2	On	2	800
5	1	210	2	90	1	Off	1	200
6	1	210	2	90	1	Off	2	800
7	1	210	2	90	2	On	1	200
8	1	210	2	90	2	On	2	800
9	2	270	1	30	1	Off	1	200
10	2	270	1	30	1	Off	2	800
11	2	270	1	30	2	On	1	200
12	2	270	1	30	2	On	2	800
13	2	270	2	90	1	Off	1	200
14	2	270	2	90	1	Off	2	800
15	2	270	2	90	2	On	1	200
$16=2^4$	2	270	2	90	2	On	2	800

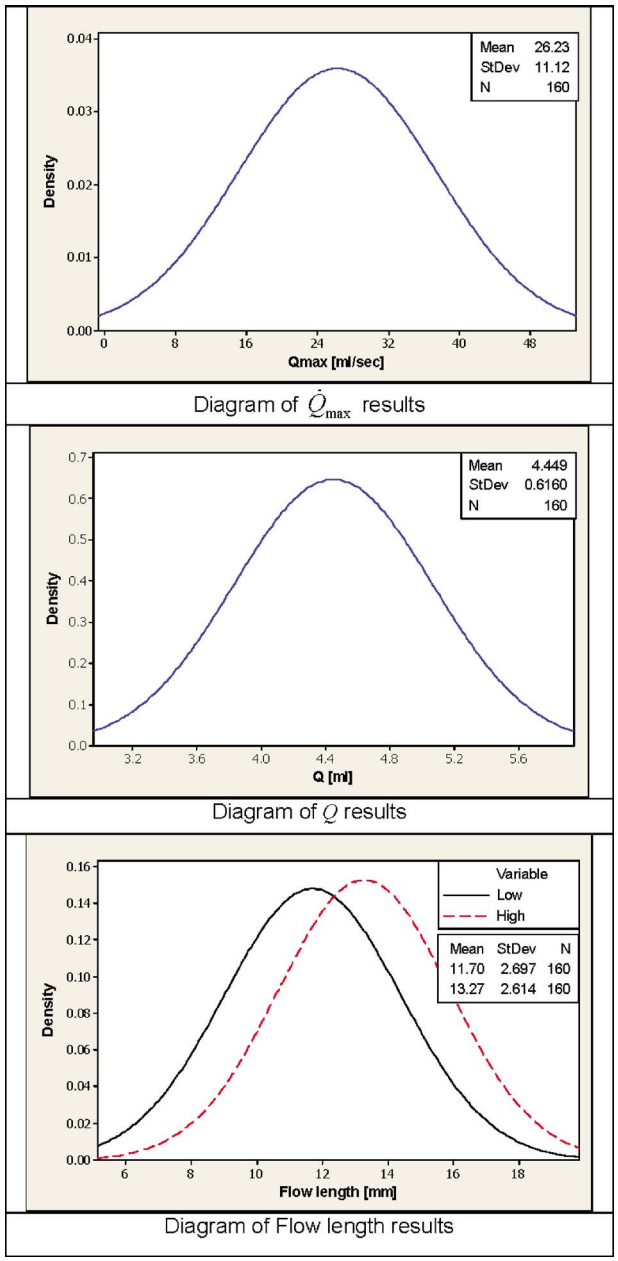

Fig. 5 Diagram of $\dot{Q}_{max}$ and Q results, and flow length results

lowest 13.8 ml/s. The normal distribution of the recorded $\dot{Q}_{max}$ shows some variation of the experimental results. In particular, Fig. 5 depicts that the average $\dot{Q}_{max}$ is 26.23 ml/s while the standard deviation (σ) was 11.12 ml/s. This result indicates that the process factors have a significant influence on $\dot{Q}_{max}$.

For the conducted trials the highest recorded Q was 5.2 ml, while the lowest was 3.6 ml. Figure 5 shows a wide variation of the results; the average Q is 4.4 ml with σ=0.61 ml. These results suggest again that the process factors have a significant influence on Q.

Regarding the flow length measurements, it was observed that they varied, too. The deviations in length for each combination of controlled parameters for each of the 16 experimental settings are given in Fig. 6. The flow front is characterized by eight individual streams resulting from the polymer flow splitting into the microchannels of the test part design. To determine the influence of the process factors on the part dimensions the highest and lowest flow stream lengths were considered, and measured for each part. The flow length measurements identify that the highest flow length stream was 18.99 mm, while the lowest was 7.66 mm. Figure 5 shows that the mean values of high and low flow lengths are 13.27 mm and 11.7 mm, respectively, while σ is 2.6 mm for both. As it was the case with Q, these results show that the process factors have also a significant influence on flow length, and that the variation in flow length for each part (experimental run) has a similar overall distribution.

4.2 Interval Plots of $\dot{Q}_{max}$, Q, and Flow Length. In this study, L16 OA was employed, and for each combination of controlled parameters ten runs were carried out and thus ten measurements of $\dot{Q}_{max}$, Q, and flow length were obtained. The mean value plots including confidence intervals are provided in Fig. 7.

The interval plots for $\dot{Q}_{max}$ identified that there is a difference; in particular, for Experiments 1–16, there is a significant variation between each consecutive experiment (Fig. 7). These changes can be explained with the variations in V_i, with low V_i resulting in low $\dot{Q}_{max}$ while high V_i leads to high $\dot{Q}_{max}$. The confidence intervals are consistent for all experiments.

The interval plots for Q in Fig. 7 showed that the variations in the experimental results are almost identical to those for $\dot{Q}_{max}$. In particular, the variations for Experiments 1–16 are similar. Also, these variations can be explained with different settings for V_i. However, there are some differences, in particular, low V_i results in high Q while low V_i leads to low $\dot{Q}_{max}$. Again, the confidence intervals are consistent for all experiments.

Finally, the analysis of the interval plots for the flow length data presented in Fig. 7 shows again variations in obtained results. In particular, for both high and low flow length measurements E_a^R was the most influential factor, with the high level of E_a^R resulting in a lower overall flow length. Generally, high V_i leads to a further reduction in the flow length. In addition, the confidence intervals for the flow length results show a wider variance than those for the mean $\dot{Q}_{max}$ and Q results.

4.3 Process Parameters' Effects on $\dot{Q}_{max}$, Q, and Flow Length. Based on the experimental results, an analysis of variance (ANOVA) was performed in order to assess the contribution of each processing parameter to the resulting $\dot{Q}_{max}$, Q, and flow rate. Table 3 and Figs. 8 and 9 show the response of each parameter and the plots of main effects, respectively.

From the $\dot{Q}_{max}$ analysis, it is immediately apparent that V_i has a strong influence on the process, and the parameter levels of T_b, T_m, and E_a^R cannot be considered as having an overall influence on the process. The results in Table 3 show that V_i is ranked as the most important factor, in particular, an increase in V_i led to an increase in $\dot{Q}_{max}$ by 143.2%. This indicates that the increase in V_i and the consequent increase in the speed of the melt flow entering the cavity contribute to an increase in the rate of E_a and hence an increase in $\dot{Q}$ through the MEMS flow sensor.

Looking at the Q results, it is immediately apparent that V_i can be considered as having the highest influence on the process. The results show that V_i is ranked the first among the controlled factors, in particular, an increase in V_i led to a decrease in Q by 23.2%. E_a^R is ranked the second as the O-ring sealing resulted in an increase in Q by 7.2%. Regarding the temperature factors, the level sets have no statistical importance on Q (Table 3). Due to the enclosed volume of air in the cavity, singling out V_i as the main factor affecting E_a is an important observation. In particular, the low level of $\dot{Q}_{max}$ when increasing V_i shows that less air was going through the MEMS flow sensor. This suggests that more air was evacuated through the primary split line vent. This is confirmed with the increase in Q when the cavity is sealed with the

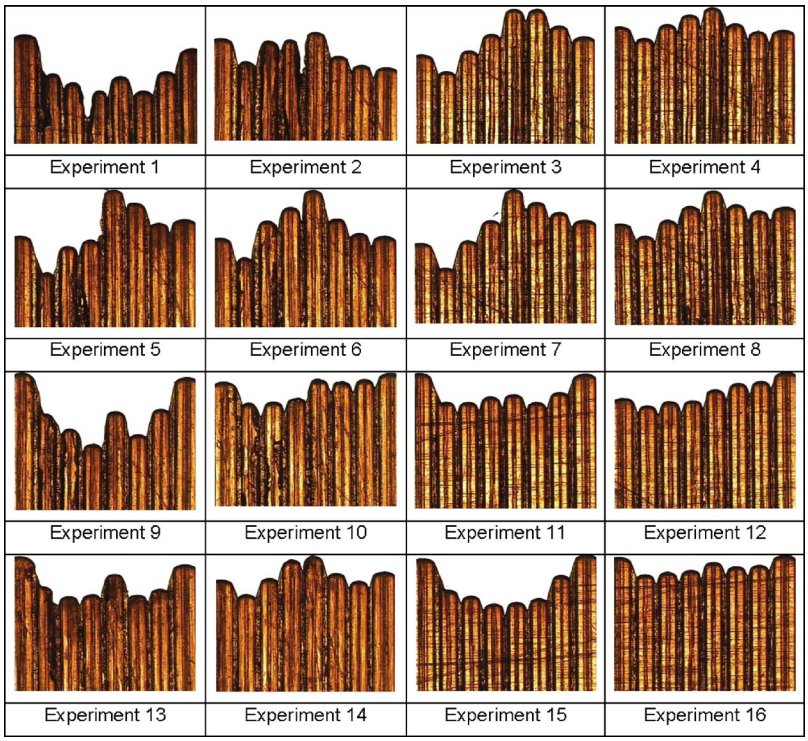

Fig. 6 Variation in the part flow length

O-ring (E_a^R), as it is shown in Fig. 8.

The part flow length for all experiments is characterized by an uneven flow front and in this research the highest and lowest flow length measurements are considered for each part. It was observed that the influence of the selected parameter levels was similar for both high and low measurements, as can be seen in Fig. 8. Also, the results show that an increase in T_B and T_m has led to an increase in the flow length, while for E_a^R the opposite has been observed. Considering the significance of different controlled factors, V_i was ranked as having the lowest statistical importance, while T_b was identified as the factor with the highest influence (Table 3). E_a^R being ranked second is of a particular interest because this parameter is not directly linked to the polymer viscosity, and thus flow mobility. The sealing of the cavity with the O-ring resulted in a decrease in the flow length by 22%, which indicates that by restricting the venting through the primary split line the resident air prevents the polymer from filling the cavity. Such a conclusion is supported by the identified relationship between V_i and E_a. V_i is ranked the most important factor for $\dot{Q}_{\max}$ and Q and as the least important one for flow length. This points out that regardless of the speed of the polymer entering the cavity the displaced air will evacuate through either primary or secondary vents or both. However, if E_a is restricted, the resident air can reduce the polymer flow length as it has been demonstrated by E_a^R in the conducted experiments.

The ANOVA analysis of the variation in flow length shows that V_i has the greatest statistical importance while T_m the least, as shown in Table 3. Additionally, by analyzing the main effects' plot for flow length variations in Fig. 9, it can be seen that in all cases the high level settings of all controlled factors resulted in a reduction in the flow length variations. However, different influences depending on the considered factors can be observed.

As far as μ-IM process factors are concerned, T_b, T_m, and V_i, high parameters' settings not only prevent an early solidification of the melt flow, i.e., promote high flow length, but also improve the evenness of the flow front (lower flow front variation). In particular, mold temperature has the least statistical significance, especially if compared with the other factors. With respect to air evacuation, the presence of the O-ring, i.e., resistance to air evacuation on, hampers the optimal filling, decreases the flow length, and also improves the filling stability, i.e., decreases flow length variation. This effect suggests that venting by using the split line of the mold leads to varying results and thus a less repeatable process. Therefore, such a venting is not suitable for precision molding of polymer microcomponents. Hence, secondary air vents coupled with vacuum technology are recommended design features to improve process performance and product quality in μ-IM.

5 Conclusion

This paper reports an experimental study on the effects of air evacuation conditions in microcavities when replicating polymer parts. To analyze the air flow state during the filling stage, a condition monitoring system was designed and integrated into the mold cavity. Then, by employing a design of experiment approach, the molding performance was studied, especially the effects of four process factors, T_b, T_m, E_a^R, and V_i, on microfeatures' flow length and air flow rates. The main conclusions made based on the obtained results are as follows.

- It is possible to assess air evacuation (E_a) conditions during part filling by employing a specially designed condition monitoring setup. It was shown that maximum air flow ($\dot{Q}_{\max}$), and air flow over time (Q) were dependent on the processing conditions.
- The data recorded for $\dot{Q}_{\max}$ and Q show a normal distribution of the experimental results. This indicates that the considered process factors have a significant influence on $\dot{Q}_{\max}$ and Q. Regarding the flow length results it was observed that the part length was not uniform. In particular, the average of high and low flow lengths shows that the process factors have a significant effect on the flow length, and that

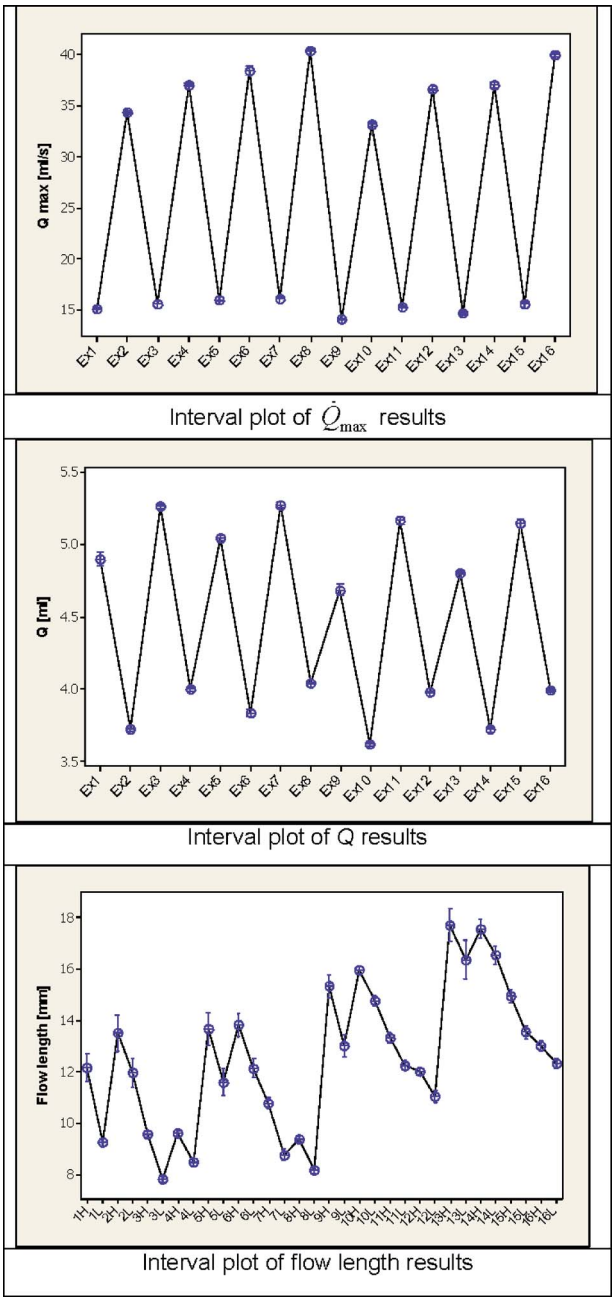

Fig. 7 Interval plot of $\dot{Q}_{max}$, Q, and flow length

the variations in the flow length for all parts have a similar distribution.

- The interval plots of the recorded $\dot{Q}_{max}$ and Q data have identified that low V_i results in low $\dot{Q}_{max}$ and high Q. The interval plots of the flow length data have identified that an increased resistance to air evacuation (E_a^R) results in a lower overall flow length.
- The parameters' effects on E_a suggest that in context to $\dot{Q}_{max}$ and Q, V_i can be considered as the most influential parameter. In particular, an increase in V_i led to an increase in $\dot{Q}_{max}$. This suggests that the increase in the speed of the polymer entering the cavity contributes to an increase in the rate of E_a. However, an increase in V_i led to a decrease in Q. This suggests that an increase in V_i results in an increased amount of E_a through the split line and not the secondary vent.
- The ANOVA analysis of the part flow length results show that an increase in T_B and T_m leads to an increase in the flow length, while for E_a^R the opposite is observed. The increase in E_a^R results in a decrease in the flow length. This indicates that a restricted venting through the primary split line results in an unevacuated resident air, which prevents the polymer from filling the cavity. This conclusion is supported by the identified dependences between V_i and $\dot{Q}_{max}$ and Q.
- The analysis of the flow length variations shows that V_i has the greatest statistical importance while T_m the least. Also, based on this analysis, it can be concluded that in all cases the high level settings of all controlled factors resulted in a reduction in the flow length variations. In addition, the high settings of T and V_i can prevent an early solidification of the melt flow and thus to improve the evenness of the flow front.

Table 3 Response table for means

Factors	T_b (°C)	T_m (°C)	E_a^R	V_i (mm/s)
		$\dot{Q}_{max}$		
Level 1	26.64	25.16	25.36	15.28
Level 2	25.81	27.29	27.09	37.17
Delta	0.83	2.13	1.73	21.89
Rank	4	2	3	1
		Q		
Level 1	4.50	4.41	4.29	5.03
Level 2	4.38	4.48	4.60	3.86
Delta	0.12	0.06	0.31	1.17
Rank	3	4	2	1
		Flow length (low)		
Level 1	9.77	11.07	13.20	11.57
Level 2	13.73	12.43	10.29	11.92
Delta	3.96	1.35	2.90	0.35
Rank	1	3	2	4
		Flow length (high)		
Level 1	11.56	12.68	14.97	13.44
Level 2	14.98	13.86	11.58	13.11
Delta	3.42	1.18	3.39	0.33
Rank	1	3	2	4
		Flow length variation		
Level 1	1.85	1.63	1.86	1.90
Level 2	1.29	1.51	1.28	1.24
Delta	0.56	0.12	0.58	0.66
Rank	3	4	2	1

By understanding the effects of V_i and E_a^R on $\dot{Q}_{max}$, Q, and the part flow length and its variations it will be possible to improve the performance of the μ-IM process. Especially, the study showed clearly that the high process settings that are required in μ-IM, together with the limited venting through the primary split line, due to the high accuracy and surface quality of used mold tools, have a significant impact on the filling performance. The extreme of this is the inability of the resident air to vent, resulting in air traps, air compression, and diesel effects, and ultimately part and mold failures. Thus, to improve the μ-IM process performance, it is necessary to incorporate in micromold tools secondary vents and vacuum methods for E_a^R.

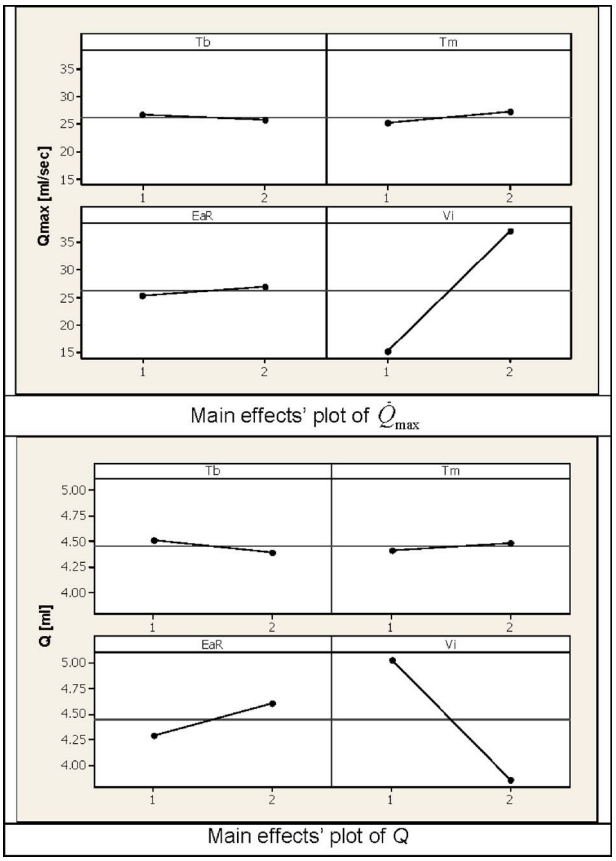

Fig. 8 Main effects' plot of $\dot{Q}_{max}$ and Q

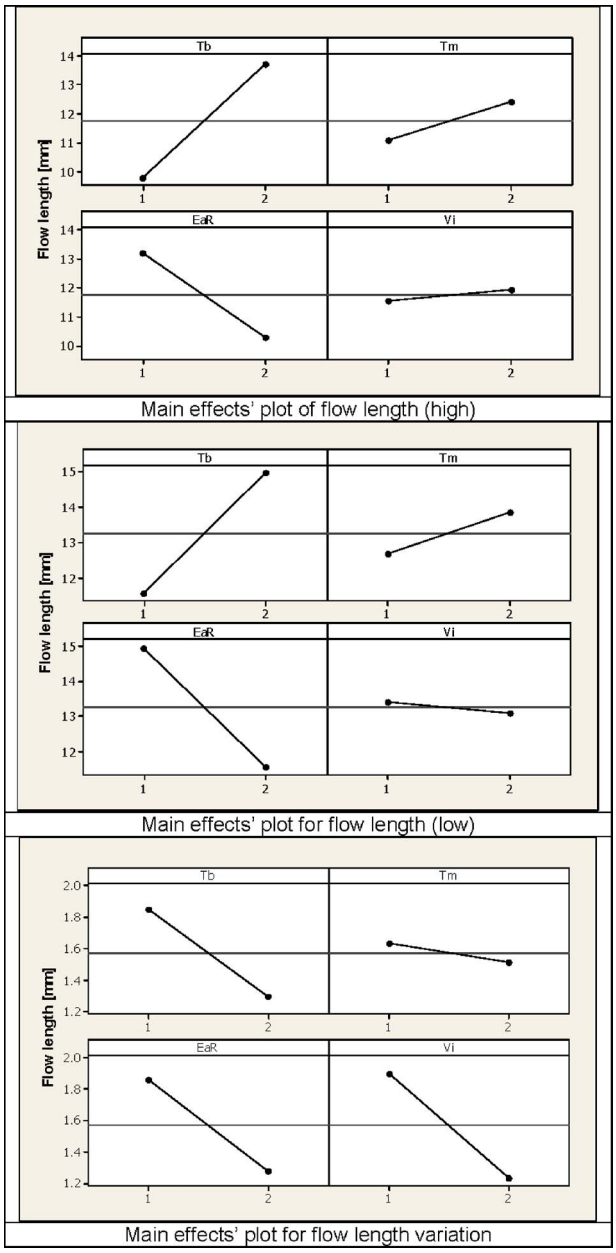

Fig. 9 Main effects' plot for the flow length

Acknowledgment

The research reported in this paper is funded by the FP7 programmes "Converging technologies for microsystems manufacturing" (COTECH, Grant Agreement No. CP-IP 214491-2, http://www.fp7-cotech.eu/) and "Integrating European research infrastructures for the micro-nano fabrication of functional structures and devices out of a knowledge-based multimaterials' repertoire" (EUMINAfab, Grant Agreement No. FP7-226460, http://www.euminafab.eu/), the U.K. Engineering and Physical Sciences Research Council (Grant No. EP/F056745/1), and the Micro-Bridge program supported by Welsh Assembly Government and the U.K. Department for Business, Enterprise and Regulatory Reform. The authors are grateful for the assistance from the Omron Corporation.

Nomenclature

E_a = air evacuation
E_a^R = resistance to air evacuation
Int_{max} = maximum integral value
P = pressure
pd(x) = probability density
P_i = injection pressure
$\dot{Q}$ = air flow rate per second
Q = air flow volume
$\dot{Q}_{max}$ = maximum air flow rate
$\dot{Q}_{start}$ = air flow rate at start
$\dot{Q}_{end}$ = air flow rate at end
SV_R = surface to volume ratio
T = temperature
t = time
T_b = melt temperature
t_h = holding pressure time
t_i = injection time
T_m = tool temperature
t_{end} = time end of air flow rate integral
t_{start} = start time
V_i = injection speed
σ = standard deviation

References

[1] Dimov, S. S., Matthew, C. W., Glanfield, A., and Dorrington, P., 2006, "A Roadmapping Study in Multi-Material Micro Manufacture," *4M 2006, Second International Conference on Multi-Material Micro Manufacture*, Elsevier, Oxford, pp. xi–xxv.
[2] Menz, W., and Dimov, S. S., 2007, "Editorial for the Special Issue of IJAMT on Multi Material Microsystem Manufacturing," Int. J. Adv. Manuf. Technol., **33**(1–2), pp. 73–74.
[3] Alting, L., Kimura, F., Hansen, H. N., and Bissacco, G., 2003, "Micro Engineering," CIRP Ann., **52**(2), pp. 635–657.
[4] Brousseau, E. B., Dimov, S. S., and Pham, D. T., 2010, "Some Recent Advances in Multi-Material Micro- and Nano-Manufacturing," Int. J. Adv.

Manuf. Technol., **47**(1–4), pp. 161–180.
[5] Kemmann, O., and Weber, L., 2001, "Simulation of the Micro Injection Molding Process," *Specialized Molding Techniques*, H.-P. Heim and H. Potente, eds., Plastic Design Library, Norwich, NY, pp. 163–169.
[6] Piotter, V., Mueller, K., Plewa, K., Ruprecht, R., and Hausselt, J., 2002, "Performance and Simulation of Thermoplastic Micro Injection Molding," Microsyst. Technol., **8**(6), pp. 387–390.
[7] Yao, D., and Kim, B., 2004, "Scaling Issues in Miniaturization of Injection Molded Parts," ASME J. Manuf. Sci. Eng., **126**(4), pp. 733–739.
[8] Kukla, C., Loibl, H., and Detter, H., 1998, *Micro-Injection Moulding, The Aims of a Project Partnership*, Kunststoffe Plastic Europe., 51, pp. 1331–1336.
[9] Fleischer, J., and Kotschenreuther, J., 2007, "The Manufacturing of Micro Molds by Conventional and Energy-Assisted Processes," Int. J. Adv. Manuf. Technol., **33**(1–2), pp. 75–85.
[10] Griffiths, C. A., Dimov, S. S., Brousseau, E. B., and Packianather, M S., 2008, "The Finite Element Analysis of Melt Flow Behaviour in Micro-Injection Moulding," Proc. Inst. Mech. Eng., Part B, **222**(9), pp. 1107–1118.
[11] Sha, B., Dimov, S., Griffiths, C., and Packianather, M. S., 2007, "Micro-Injection Moulding: Factors Affecting the Achievable Aspect Ratios," Int. J. Adv. Manuf. Technol., **33**(1), pp. 147–156.
[12] Wimberger-Friedl, R., 2001, "Injection Molding of Sub-μm Grating Optical Elements," *Specialized Molding Techniques*, H.-P. Heim and H. Potente, eds., Plastic Design Library, Norwich, NY, pp. 149–155.
[13] Tosello, G., 2008, "Precision Moulding of Polymer Micro Components-Optimization, Simulation, Tooling, Quality Control and Multi-Material Application," Ph.D. thesis, Department of Mechanical Engineering, Technical University of Denmark, Kgs. Lyngby, Denmark.
[14] Tosello, G., Gava, A., Hansen, H. N., and Lucchetta, G., 2010, "Study of Process Parameters Effect on the Filling Phase of Micro-Injection Moulding Using Weld Lines as Flow Markers," Int. J. Adv. Manuf. Technol., **47**(1–4), pp. 81–97.
[15] 1965, *The Principles of Injection Moulding*, ICI Plastics Technical Service, Welwyn Garden City, Herts.
[16] Su, Y.-C., Shah, J., and Lin, L., 2004, "Implementation and Analysis of Polymeric Microstructure Replication by Micro Injection Molding," J. Micromech. Microeng., **14**(3), pp. 415–22.
[17] 1993, *How to Make Injection Molds*, G. Menges and P. Mohren, eds., Hanser Publisher, Munich, Vienna, New York.
[18] Crawford, R. J., 1990, *Plastics Engineering*, 2nd ed., Pergamon, New York.
[19] Yokoi, H., Masuda, N., and Mitsuhata, H., 2002, "Visualization Analysis of Flow Front Behavior During Filling Process of Injection Mold Cavity by Two-Axis Tracking System," J. Mater. Process. Technol., **130–131**, pp. 328–333.
[20] Roopesh, M., Suresh, A. G., and Fink B. K., 2004, 2004, "Use of Genetic Algorithms to Optimise Gate and Vent Locations for the Resin Transfer Molding Process," Polym. Compos., **20**(2), pp. 167–178.
[21] Phelan, F. R., 1997, "Simulation of the Injection Process in Resin Transfer Moulding," Polym. Compos., **18**(4), pp. 460–476.
[22] Shen, Y. K., Chang, C. Y., Shen, Y. S., Hsu, S. C., and Wu, M. W., 2008, "Analysis for Microstructure of Microlens Arrays on Micro-Injection Molding by Numerical Simulation," Int. Commun. Heat Mass Transfer, **35**(6), pp. 723–727.
[23] Bendada, A., Derdouri, A., Lamontagne, M., and Simard, Y., 2004, "Analysis of Thermal Contact Resistance Between Polymer and Mold in Injection Molding," Appl. Therm. Eng., **24**(14–15), pp. 2029–2040.
[24] Zauner, R., 2006, "Micro Powder Injection Moulding Microelectronic Engineering," Microelectron. Eng., **83**(4–9), pp. 1442–1444.
[25] Yokoi, H., Han, X., Takahashi, T., and Kim, W. K., 2006, "Effects of Molding Conditions on Transcription Molding of Microscale Prism Patterns Using Ultra-High-Speed Injection Molding," Polym. Eng. Sci., **46**(9), pp. 1140–1146.
[26] Kalima, V., Pietarinen, J., Siitonen, S., Immonen, J., Suvanto, M., Kuittinen, M., Mönkkönend, K., and Pakkanen, T. T., 2007, "Transparent Thermoplastics: Replication of Diffractive Optical Elements Using Micro-Injection Molding," Opt. Mater. (Amsterdam, Neth.), **30**(2), pp. 285–291.
[27] Liou, A.-C., and Chen, R.-H., 2006, "Injection Molding of Polymer Micro- and Sub-Micron Structures With High-Aspect Ratios," Int. J. Adv. Manuf. Technol., **28**(11–12), pp. 1097–1103.
[28] Dairanieh, I. S., Haufe, A., Wolf, H. J., and Mennig, G., 1996, "Computer Simulation of Weld Lines in Injection Molded Poly(Methyl Methacrylate)," Polym. Eng. Sci., **36**(15), pp. 2050–2057.
[29] Kim, J. K., Song, J. H., Chung, S. T., and Kwon, T. H., 1997, "Morphology and Mechanical Properties of Injection Molded Articles With Weld-Lines," Polym. Eng. Sci., **37**(1), pp. 228–241.
[30] Debondue, E., Fournier, J.-E., Lacrampe, M.-F., and Krawczak, P., 2004, "Weld-Line Sensitivity of Injected Amorphous Polymers," J. Appl. Polym. Sci., **93**(2), pp. 644–650.
[31] Michaeli, W., and Ziegmann, C., 2003, "Micro Assembly Injection Moulding for the Generation of Hybrid Microstructures," Microsyst. Technol., **9**(6–7), pp. 427–430.
[32] Liu, S.-J., Wu, J.-Y., Chang, J.-H., and Hung, S.-W., 2000, "An Experimental Matrix Design to Optimize the Weldline Strength in Injection Molded Parts," Polym. Eng. Sci., **40**(5), pp. 1256–1262.
[33] Wu, C.-H., and Liang, W.-J., 2005, "Effects of Geometry and Injection-Molding Parameters on Weld-Line Strength," Polym. Eng. Sci., **45**(7), pp. 1021–1030.
[34] Chang, R. Y., Chen, C. H., and Su, K. S., 1996, "Modifying the Tait Equation With Cooling-Rate Effects to Predict the Pressure-Volume-Temperature Behaviors of Amorphous Polymers: Modeling and Experiments," Polym. Eng. Sci., **36**(13), pp. 1789–1795.
[35] Binet, C., Heaney, D. F., Spina, R., and Tricarico, L., 2005, "Experimental and Numerical Analysis of Metal Injection Molded Products," J. Mater. Process. Technol., **164–165**, pp. 1160–1166.
[36] Giboz, J., Copponnex, T., and Mele, P., 2007, "Microinjection Molding of Thermoplastic Polymers: A Review," J. Micromech. Microeng., **17**(6), pp. R96–V109.
[37] 2003, *McGraw-Hill, Dictionary of Engineering*, 2nd Ed., McGraw-Hill, New York.
[38] Moran, M. J., 1999, "Engineering Thermodynamics," *Mechanical Engineering Handbook*, F. Kreith, ed., CRC, Boca Raton, FL.
[39] Young, W. B., 2005, "Effect of Process Parameters on Injection Compression Molding of Pickup Lens," Appl. Math. Model., **29**(10), pp. 955–971.
[40] Griffiths, C. A., Dimov, S. S., Brousseau, E. B., and Hoyle, R. T., 2007, "The Effects of Tool Surface Quality in Micro-Injection Moulding," J. Mater. Process. Technol., **189**(1–3), pp. 418–427.
[41] Sha, B., Dimov, S. S., Griffiths, C. A., and Packianather, M. S., 2007, "Investigation of Micro-Injection Moulding: Factors Affecting the Replication Quality," J. Mater. Process. Technol., **183**(2–3), pp. 284–296.
[42] Yuan, S., Hung, N. P., Ngoi, B. K. A., and Alia, M. Y., 2003, "Development of Microreplication Process—Micromolding," Mater. Manuf. Processes, **18**(5), pp. 731–751.
[43] Ruprecht, R., Gietzelt, T., Müller, K., Piotter, V., and Haußelt, J., 2008, "Injection Molding of Microstructured Components From Plastics, Metals and Ceramics," Microsyst. Technol., **8**(4–5), pp. 351–358.
[44] Ebnesajjad, S., 2003, *Fluoroplastics, Volume 2: Melt Processible Fluoroplastics: The Definitive User's Guide*, William Andrew Publishing/Plastics Design Library, Norwich, NY.
[45] 2003, *Dictionary of Scientific & Technical Terms*, McGraw-Hill, New York.